



Paired Synoptic and Long-Term Monitoring Datasets Reveal Decadal Shifts in Suspended Sediment Supply and Particulate Organic Matter Sources in a River-Estuarine System

C. M. Richardson¹ · M. Young² · A. Paytan³

Received: 19 August 2022 / Revised: 7 December 2022 / Accepted: 9 December 2022 / Published online: 8 February 2023
© The Author(s) 2023

Abstract

The San Francisco Estuary, in central California, has several long-running monitoring programs that have been used to reveal human-induced changes throughout the estuary in the last century. Here, we pair synoptic records of particulate organic matter (POM) composition from 1990–1996 and 2007–2016 with more robust long-term monitoring program records of total suspended sediment (TSS) concentrations generally starting in the mid-1970s to better understand how POM and TSS sources and transport have shifted. Specifically, POM C:N ratios and stable isotope values were used as indicators of POM source and to separate the bulk POC pool into detrital and phytoplankton components. We found that TSS and POC sources have shifted significantly across the estuary in time and space from declines in terrestrial inputs. Landward freshwater and brackish water sites, in the Delta and near Suisun Bay, witnessed long-term declines in TSS (32 to 52%), while seaward sites, near San Pablo Bay, recorded recent increases in TSS (16 to 121%) that began to trend downwards at the end of the record considered. Bulk POM C:N ratios shifted coeval with the TSS concentration changes at nearly all sites, with mean declines of 12 to 27% between 1990–1996 and 2007–2016. The widespread declines in bulk POM C:N ratios and inferred changes in POC concentrations from TSS trends, along with the substantial declines in upstream TSS supply through time (56%), suggest measurable reductions in terrestrial inputs to the system. Changes in terrestrial TSS and POM inputs have implications for biotic (e.g., food web dynamics) and abiotic organic matter cycling (e.g., burial, export) along the estuarine continuum. This work demonstrates how human-generated environmental changes can propagate spatially and temporally through a large river-estuary system. More broadly, we show how underutilized monitoring program datasets can be paired with existing (and often imperfect) synoptic records to generate new system insight in lieu of new data collection.

Keywords Estuary · Detritus · Rivers · Environmental change · Carbon · Data synthesis

Introduction

Estuaries are especially susceptible to human impacts due to their direct hydrologic connection to both marine and riverine systems (Cloern et al. 2016). Particulate organic matter

(POM), a key component of aquatic food webs in estuaries, likely responds to these interacting riverine, marine, and anthropogenic drivers. Changes in estuarine POM quantity and quality are difficult to detect and track through time, however, due in large part to a paucity of long-term monitoring data as well as the inherent biogeochemical and hydrological complexity of these sites that often limits interpretations to the synoptic windows of which the measurements were made in. As a result, key questions remain about how estuarine POM responds to different modes of anthropogenic alteration, which can propagate through systems as changes in organic matter (OM) sources and cycling.

Bulk POM in river deltas and connected coastal estuaries can originate from a complex mixture of sources (e.g., phytoplankton, microzooplankton, bacteria, aquatic macrophytes, and terrestrial soil/vegetation). The quality of bulk

Communicated by Neil Kamal Ganju.

✉ C. M. Richardson
cmrichar@ucsc.edu

¹ Earth and Planetary Sciences, University of California at Santa Cruz, 1156 High Street, Santa Cruz, CA 95064, USA

² Water Mission Area Laboratory & Analytical Services Division, U.S. Geological Survey, Menlo Park, CA, USA 94025

³ Institute of Marine Sciences, University of California at Santa Cruz, Santa Cruz, CA 95064, USA

POM, in terms of its nutritional value and preference for consumption by higher-level organisms, like zooplankton or clams, and thus incorporation into the food web, can range considerably, depending on the dominant source (Canuel et al. 1995; Canuel and Hardison 2016; Müller-Solger et al. 2002). For example, allochthonous sources of detritus, like terrestrial soil and vegetation, typically comprise a large fraction of the bulk POM pool in freshwater systems and estuaries, but are thought to be of low nutritional quality, with little protein and no polyunsaturated fatty acids that are critical for zooplankton metabolism (Hixson et al. 2015). More recent work suggests that terrestrial POM may actually be important supplementary food sources for estuarine zooplankton (Harfmann et al. 2019). In estuarine systems, bulk POM typically shifts from such allochthonous dominant contributions in low salinity headwaters to autochthonous dominant inputs in the brackish waters downstream (Canuel and Hardison 2016). The autochthonous POM pool is sustained by microbial biomass and phytoplankton primary production, the relative contribution of which can vary significantly across the world's river deltas and estuaries, though most are classified as net heterotrophic (Caffrey 2004; Cloern et al. 2014).

Physical and biogeochemical controls on allochthonous and autochthonous OM sources and transformations are complex. As systems connected to rivers and oceans, OM concentration and composition in estuaries reflect the integration of a variety of biotic (e.g., microbial degradation, uptake) and abiotic (e.g., sorption/desorption, photo oxidation, burial/re-suspension) processes that imprint and/or alter primary source materials (Canuel and Hardison 2016). Annual variability in freshwater inflow and sub-seasonal variability in event flow from rainfall/snowmelt can drastically alter (1) sediment and associated OM inputs for systems downstream, like estuaries, and (2) the residence time of water, which impacts estuarine OM transport and cycling (Middelburg and Herman 2007). Other physical controls on transport, like tidal currents and wind-wave resuspension, become increasingly important as systems transition along the river to the estuary continuum (Barnard et al. 2013). Similarly, processes that affect internal OM generation and degradation, like primary productivity and respiration, can be affected by a range of physicochemical factors (e.g., turbidity, nutrient availability, temperature, oxygenation), many of which have been altered by human activities (Cloern and Jassby 2012; Jaffe et al. 2007). Here, we leverage multiple existing datasets to examine how sediment supply and related POM quantity and quality have shifted over the course of nearly half a century along a roughly 160-km stretch of the human-impacted San Francisco Estuary (SFE) that spans from fresh river waters (an area encompassing the Sacramento-San Joaquin Delta, hereafter “the Delta”) to near marine bay waters (San Francisco Bay, hereafter “SF Bay”). The datasets, which are at different sampling frequencies and temporal resolution, provide

insight and supporting evidence for long-term environmental change. We highlight this feature to emphasize (1) the importance of examining similar imperfect and underutilized existing datasets in other systems in lieu of new data collection where appropriate, and (2) to support analysis of new datasets that may lack historical context.

Modern day declines in phytoplankton primary productivity in the SFE place this system in the bottom half of global estuaries with respect to primary production levels (Cloern et al. 2014). Recent estimates suggest related microalgae and marsh plant contributions to net primary productivity, once the dominant primary producer groups in the Delta, have decreased significantly since the 1800s due to expansive wetland habitat loss (Cloern et al. 2021). Widespread growth of aquatic plants, many of which are invasive, have also helped to shift the relative importance of different primary producer groups in the freshwater portions of the SFE (Ta et al. 2017). Declines in phytoplankton production affect in situ and downstream autochthonous POM supply. Less is known about how the allochthonous POM supply has shifted in the SFE, though the relationship between this pool and total suspended sediment (TSS) supply suggests that similar declines have occurred. As few long-term records of POM quality and quantity exist for systems spanning freshwater-estuarine gradients, proxies for POM that share similar transport and mobilization pathways, like TSS, can be useful for general inferences. TSS and POC concentrations are broadly and generally strongly positively correlated in the SFE (Hernes et al. 2020), even amongst historical data from several decades ago (Cloern et al. 1993).

Sediment supply in the SFE has drastically changed in the past century (Barnard et al. 2013). While TSS inputs from large rivers in the Delta once accounted for the majority of SF Bay sediment loads, McKee et al. (2013) found that TSS loads in the SFE are now commonly dominated by tributary inputs from small watersheds downstream of the Delta. This shift from large to small river dominance is thought to be tied to the exhaustion of the sediment supply produced from hydraulic mining during the Gold Rush as well as enhanced sediment retention by flood control bypasses, riverbank armoring, and upstream dams on the larger rivers that drain into the Delta (Schoellhamer 2011). As a result, TSS concentrations in the Sacramento River, the largest freshwater source in this system, have declined by roughly 50% between the 1950s and early 2000s (Wright and Schoellhamer 2004). Sediment deposition rates in the Delta are also thought to have declined (Canuel et al. 2009). These long-term decreases in upstream TSS inputs are likely reflected in changes in POM dynamics in the SFE due to similarities in sourcing and transport mechanisms.

More recent synoptic work suggests that bulk POM quality in this system has shifted. Hernes et al. (2020) found

evidence of lower bulk POM C:N ratios at present when comparing to synoptic historical data in the north SF Bay. Shifts in C:N ratios hint at larger-scale changes in sources and biological and/or physical processes. To build on this recent work, we leverage both historical and modern POM data and pair it with existing records of related water quality parameters, with a focus on TSS, to examine how POM sources have shifted across time and space in the SFE (Fig. 1).

Study Area

Sacramento-San Joaquin Delta

The Delta drains nearly 40% of California's land area, with the Sacramento and San Joaquin rivers accounting for most of the freshwater entering this system. Nearly 70% of all sediment entering the Delta is deposited before reaching the SF Bay (Wright and Schoellhamer 2005). Sediment delivery is often driven by episodic events during the rainy season. Wright and Schoellhamer (2005) found that roughly 80% of sediment is delivered during about 3 months of the year.

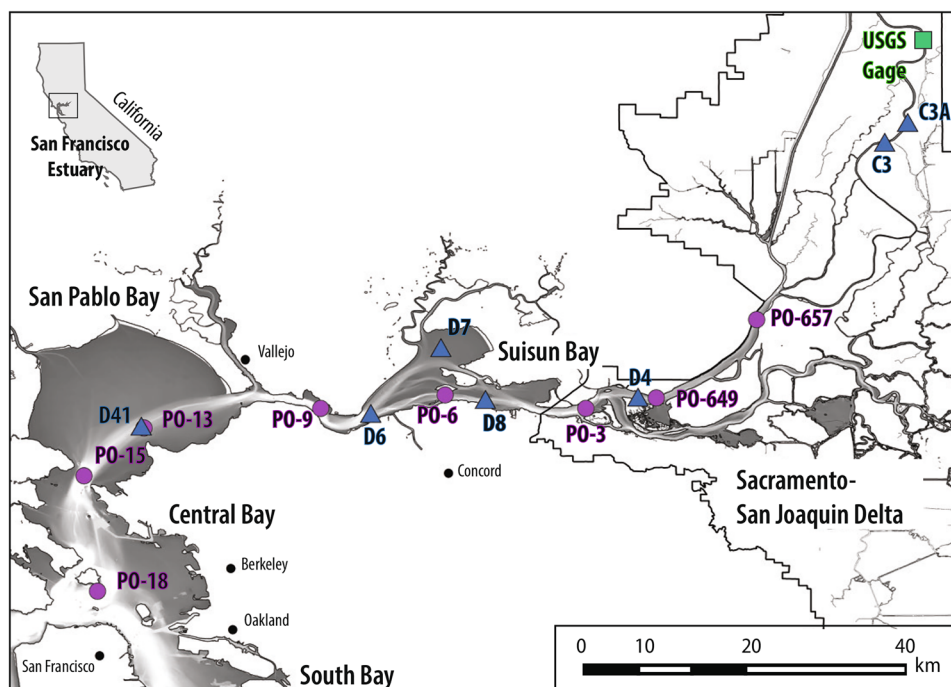
San Francisco Bay

Suspended sediment dynamics are spatially variable within the four different subembayments (Suisun Bay, San Pablo Bay, Central Bay and South Bay) of the San Francisco Bay. Complex

seaward and landward controls can lead to net erosional or depositional microenvironments across the subembayments. In dry water years (a water year is defined as the period from October 1 to September 30 and named for the calendar year in which it ends) with low discharge from the Delta's large rivers, sediment is imported from both land- and seaward boundaries in Suisun Bay, leading to net deposition of sediment (Schoellhamer 2011). This cross-source sediment supply is important to emphasize as it directly relates to the POM supply. Only a fraction of the suspended sediment supply entering the Delta is estimated to remain entrained and enter Suisun Bay (Wright and Schoellhamer 2005). San Pablo Bay is just downstream of Suisun Bay; thus, it has a stronger hydrologic connection to the marine environment and is more saline. Both Suisun and San Pablo Bays have a narrow deep-water navigation channel that runs through them, with shallower fringing marsh and wetland environments surrounding large regions of the shoreline. San Pablo Bay commonly supplies sediment to the landward Carquinez Strait, mostly during low-flow months when freshwater outflow is limited, and tidal forcing controls the direction of total water flux. The Central Bay connects the SFE to the ocean and is a near marine environment with hardened shorelines and several deep-water shipping channels running through it.

Temporal and spatial controls on TSS in the four subembayments are complex. Sediment loads from small tributaries that drain into the SF Bay, without passing through the Delta, are now just as important to SF Bay sediment budgets as upstream sediment inputs from the Delta. Similar to

Fig. 1 Study area showing the Sacramento-San Joaquin Delta and different embayments of the San Francisco Bay (Suisun Bay, San Pablo Bay, Central Bay, and South Bay). The California Department of Water Resources Interagency Ecological Program's Environmental Monitoring Program (DWR IEP EMP) sites used in this study are shown as blue triangles. The U.S. Geological Survey's San Francisco Bay Regional Monitoring Program (USGS SFB RMP) sites used in this study are shown as purple circles. The USGS Station 11447650 (Sacramento River at Freeport) gage site is shown as a green square. Water depth is qualitatively shown as grey (shallower) to white (deeper) shading for reference



sediment dynamics in the Delta, large pulses of sediment during the winter rainy season dominate the sediment supply. McKee et al. (2006) show that more than 40% of the annual sediment load of the SF Bay can be delivered over the course of just seven days during exceptionally wet years, though this response may be dampening based on the more recently documented declines in SF Bay TSS concentrations (Schoellhamer 2011). In addition to inputs from rivers, physical controls on transport shift along the freshwater-estuarine continuum. While sediment dynamics at freshwater sites are primarily controlled by freshwater inflow, a range of variables, that include processes like tidal pumping and wind-wave resuspension, gain importance with increasing proximity to the marine environment.

Methods

Data Sources

Two existing inter-agency long-term monitoring program datasets were used to examine how POM and related water quality variables (primarily TSS) in the SFE have shifted: (1) the U.S. Geological Survey's San Francisco Bay Research and Monitoring Project (SFB RMP) (data availability and methods summarized by Schraga and Cloern (2017)) and (2) the Interagency Ecological Program Environmental Monitoring Program (IEP EMP) (see <https://iep.ca.gov/Science-Synthesis-Service/Monitoring-Programs/EMP>).

POM stable isotope data, which were collected in conjunction with the SFB RMP at irregular intervals during several water years (2007, 2008, 2011, 2012, 2013, 2014, 2015, and 2016) were also used. For insight into historical POM quality, we compiled POM stable isotope data and select associated sterol concentrations from these cruises in the early 1990s as published in Canuel et al. (1995); stable isotope data spanned six dates across the 1990, 1991, and 1992 water years, and sterol concentrations were only available for one sampling event in March 1991. Additional historical records, from many of these same sites, were pulled from Murrell et al. (1999) where data irregularly covered April through October of 1996.

For all the SFB RMP datasets, we focused on sites in the Delta and north SF Bay where both POM stable isotope data and complimentary nutrient/other water quality parameter data were available: PO-657, PO-653, PO-3, PO-6, PO-9, PO-13, PO-15, and PO-18 (Fig. 1). Additionally, as not all sites had data available for the historical period, we used neighboring sites (for ex., PO-4, PO-8, etc.) to improve our historical database. POC concentrations for the modern POM dataset were calculated from TSS concentrations using the regression equation from Hernes et al. (2020). We first

ground-truthed these estimates with historical POC concentration data from Cloern et al. (1993); POC concentrations were only slightly underestimated ($\text{POC}_{\text{actual}} = 1.16 * \text{POC}_{\text{est}}$, $R^2 = 0.79$). We also used this regression to compare predicted POC to actual PC concentrations from a more recent unpublished SF RMP dataset (2016 to 2020, $n = 78$) from several of the same sites considered herein (PO-657, PO-649, PO-6, PO-13, PO-18); predicted concentrations lined up well with actual PC data ($\text{PC}_{\text{actual}} = 1.01 * \text{POC}_{\text{est}}$, $R^2 = 0.87$). These comparisons show that the regression used is a relatively robust predictor of POC concentrations across the times and locations considered in the north SF Bay and Delta.

Due to the non-continuous nature of early records from the SFB RMP, we complemented the SFB RMP data with IEP EMP data. We focus on IEP EMP sites C3/3a, D4, D6, D7, D8, and D41, which generally cover the same regions of the SFE as the SFB RMP transects (Fig. 1). The IEP EMP has more complete historical records of water quality that started in 1975 to 1980, and, as such, we used the IEP EMP data to provide important long-term context for the synoptic POM datasets.

Assessing Long-Term Changes in Riverine TSS Concentrations and Fluxes

For insight into long-term changes in riverine TSS dynamics, we analyzed flow and TSS data from U.S. Geological Survey Station 11447650 (Sacramento River at Freeport) using the Weighted Regressions on Time, Discharge, and Season (WRTDS) model (Hirsch et al. 2010). TSS and daily flow data were examined from 1956 to 2020. TSS samples were collected generally daily starting in 1962. Prior to 1962, samples were collected between 3 to 31 times every month. WRTDS is commonly used to evaluate long-term changes in concentrations and fluxes of water quality parameters of interest. In the absence of high-frequency water quality data, WRTDS offers methodical advantages over more traditional models, like LOADEST, that can improve flux estimates (Moyer et al. 2012). Model fit, based on the flux bias statistic (FBS) defined as:

$$\text{FBS} = (\text{mean}_{\text{pred}} - \text{mean}_{\text{obs}}) / \text{mean}_{\text{obs}}$$

where $\text{mean}_{\text{pred}}$, which is the mean of the predicted flux, and mean_{obs} , which is the mean of the observed flux, was -0.085 . Hirsch (2014) considers acceptable FBS values of ± 0.100 . WRTDS produces estimates of TSS concentrations and fluxes as well as flow-normalized TSS concentrations and fluxes. Flow-normalized TSS concentrations and fluxes remove the temporal influence of discharge and are further described in Hirsch et al. (2010).

Calculations for Separating the Bulk POC Pool into Phytoplankton and Detrital Components

Bulk POC concentrations, POM C:N molar (C:N)_m, ratios, and $\delta^{13}\text{C}$ -POC values were partitioned into detrital and phytoplankton components by leveraging existing data. We estimated phytoplankton carbon biomass by assuming a C:Chl. *a* ratio of 35, like other studies in this system (Cloern et al. 1995; Hernes et al. 2020; Sobczak et al. 2005). Phytoplankton signatures were removed from the bulk POM C:N pool by assuming that phytoplankton C:N ratios were 6.6 for data with salinities below 5 and 6 when salinities were above 5 based on phytoplankton C:N data from Cloern et al. (2002). Detrital C:N ratios were then solved for using a simple mass balance:

$$\text{C:N}_{\text{detritus}} = ((\text{POC}_{\text{bulk}} \cdot \text{C:N}_{\text{bulk}}) - (\text{POC}_{\text{phyto}} \cdot \text{C:N}_{\text{phyto}})) / (\text{POC}_{\text{detritus}})$$

$\delta^{13}\text{C}$ -phytoplankton values were estimated from $\delta^{13}\text{C}$ -POC values using coeval dissolved inorganic carbon (DIC) stable isotope data. First, we used seasonal relationships between salinity (S) and $\delta^{13}\text{C}$ -DIC values to predict $\delta^{13}\text{C}$ -DIC values for any missing time periods (summer, $0.27 \cdot \text{S} - 9.2$, $R^2 = 0.94$; fall, $0.27 \cdot \text{S} - 10.1$, $R^2 = 0.68$; winter, $0.30 \cdot \text{S} - 10.4$, $R^2 = 0.90$; spring, $0.32 \cdot \text{S} - 10.3$, $R^2 = 0.94$); salinity and $\delta^{13}\text{C}$ -DIC values in this system are generally closely correlated as salinity is a relative proxy for freshwater versus marine inorganic carbon sources, which have distinct endmember values. We approximated an enrichment factor for phytoplankton C fixation using historical $\delta^{13}\text{C}$ -phytoplankton data for freshwater ($-28.4 \pm 1.2\text{‰}$) and estuarine-marine ($-21.5 \pm 2.9\text{‰}$) phytoplankton from Cloern et al. (2002) in conjunction with $\delta^{13}\text{C}$ -DIC values from this study. For freshwater dominant sites, we averaged the DIC data from this study that overlapped with the freshwater transect from Cloern et al. (2002); the mean $\delta^{13}\text{C}$ -DIC value across the four overlapping sites (PO-657, PO-649, PO-3, and PO-6) was $-8.8 \pm 1.6\text{‰}$. Since limited DIC data was available for the more brackish and marine water region where the estuarine-marine phytoplankton samples were collected, we assumed the marine $\delta^{13}\text{C}$ -DIC value was close to -1.5‰ to reference to the estuarine-marine phytoplankton data. Based on differences between $\delta^{13}\text{C}$ -DIC and $\delta^{13}\text{C}$ -phytoplankton values discussed above, we assumed an approximate enrichment factor of -20‰ to represent C uptake by phytoplankton. Then, using the enrichment factor of -20‰ , we were able to estimate $\delta^{13}\text{C}$ -phytoplankton ($\delta^{13}\text{C}_{\text{phyto}}$) values. With $\delta^{13}\text{C}$ -phytoplankton values and bulk $\delta^{13}\text{C}$ -POC values, $\delta^{13}\text{C}$ -detritus values were solved for simply via mass balance:

$$\delta^{13}\text{C}_{\text{detritus}} = ((\text{POC}_{\text{bulk}} \cdot \delta^{13}\text{C}_{\text{bulk}}) - (\text{POC}_{\text{phyto}} \cdot \delta^{13}\text{C}_{\text{phyto}})) / (\text{POC}_{\text{detritus}})$$

Data Processing and Analysis

Statistical analyses were performed using the *wql* package in R (Jassby and Cloern 2010). Mann–Kendall tests were performed on annualized IEP EMP time series data, and Seasonal Kendall tests were performed on monthly IEP EMP time series data. These tests measure trends of change over time, and both scales can provide useful information about long-term change. We also examined decadal-scale oscillations in IEP EMP time series data using rolling Seasonal Kendall tests in *wql* package, which can be useful for examining cycles of trends that stretch beyond single-year increments (Cloern 2019).

Results

Long-Term Changes in Riverine TSS Exports

TSS concentrations and fluxes declined over the past ~70 years (Fig. 2, Table 1). While some of the change was driven by hydrologic variability across water years, as evidenced by the TSS concentration shifts across decades, flow-normalized TSS concentrations showed similar declines of 55%. Mean flow normalized TSS concentrations decreased from $86.8 \pm 6.3 \text{ mg L}^{-1}$ in the 10-yr window of 1956–1965 to $38.4 \pm 4.8 \text{ mg L}^{-1}$ between 2006–2020. Both TSS fluxes and flow normalized TSS fluxes also declined, by close to 57%, since the first records began at this site in 1956–1965.

Spatial and Temporal Changes in Estuarine TSS

Since 1975, TSS concentrations have measurably shifted across the SFE. Fresh- and mid-salinity sites experienced declines in TSS, while more western marine sites recorded recent increases in TSS (Figs. 3 and 4). In the northeastern region of the SFE, at the freshwater site (C3/C3a), decadal mean TSS concentrations decreased from 27.5 to 18.6 mg L^{-1} across the binned decades spanning 1975–2020 (Table 2). Trend tests showed statistically significant trends in TSS ($p < 0.06$) on the annualized time series data at C3 (Table 3), and both seasonal means across decades and annual trends indicated declines. Downstream sites in low- to mid-salinity zones (D4, D7, and D8) also showed declines in decadal mean TSS concentrations, with absolute declines of over 20 mg L^{-1} that equated to a reduction of 32 to 52% over the time periods of 1975–1985 to 2005–2020. These changes were supported by trend tests, which showed statistically significant annual declines of 0.44 to 0.57 mg L^{-1} at sites D4, D7, and D8 ($p < 0.05$, Table 2). Downstream of these sites, at

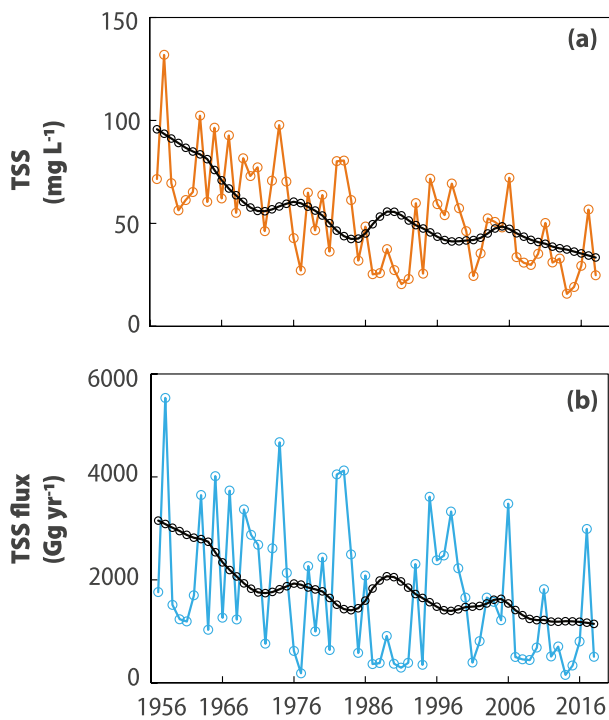


Fig. 2 Long-term changes in (a) TSS concentrations and (b) TSS fluxes at the Sacramento River at Freeport (USGS Station 11447650). Colored lines show annual absolute concentrations or fluxes. Black lines and circular markers indicate (a) flow-normalized TSS concentrations, and (b) flow-normalized TSS fluxes

D6 and D41 in the Carquinez Strait and San Pablo Bay, trends in decadal mean TSS concentrations reversed in direction and increased by 4 and 13.5 mg L⁻¹ in absolute terms or roughly 16 to 121%, respectively. These increases equated to statistically significant annual TSS increases of 0.24 to 0.44 mg L⁻¹ per year (*p* < 0.05), though the largest period of increase appeared to be relatively recent, from 2006–2020.

Changes through time and space were not static across months or years. Seasonal means by decade, along with seasonal trend analyses, provided additional insight into

periods of the year seeing the greatest changes in space and time. Seasonal mean TSS concentrations declined the most during winter at the more freshwater sites, C3/3A and D4 (Table 2). For other regions of the SFE, spring, summer, and fall months generally showed the greatest absolute change, during which TSS concentrations declined at freshwater and brackish sites (D4, D8, and D7) and increased at more marine sites (D6, D41) (Table 2). Seasonal Kendall tests also showed that summer periods accounted for some of the greatest periods of change across sites in the low to mid-salinity zones (D4, D7, and D8) (Fig. 5a). Decadal trends oscillated across the period of record at each site, with some overall spatial consistencies in direction but not magnitude, aside from the freshwater site (C3/3A) which was slightly decoupled from downstream dynamics (Fig. 5b).

Spatial and Temporal Changes in Estuarine POM

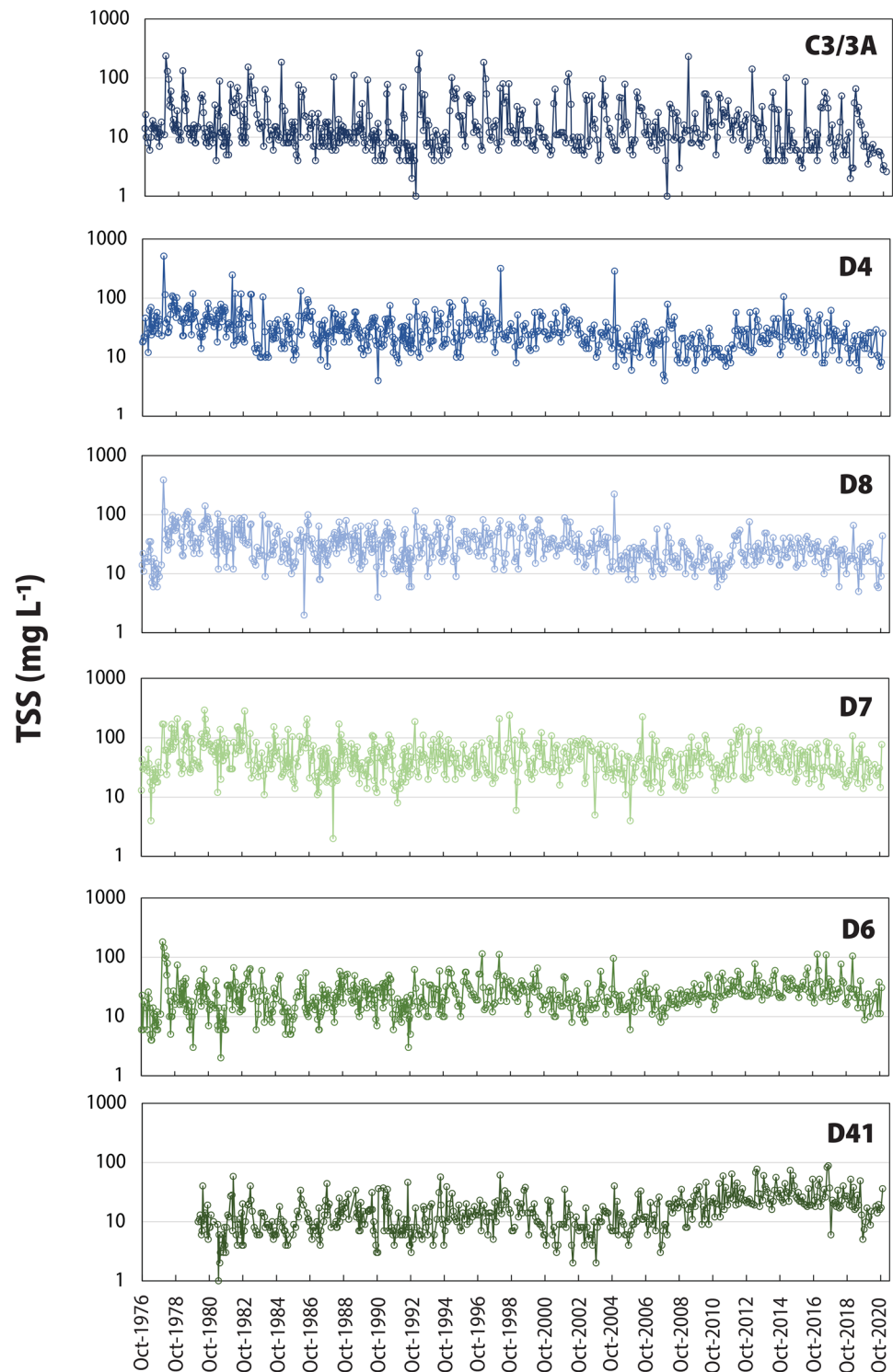
Mean annual bulk POC concentrations and mean bulk POM C:N ratios from 1990 to 1992 across all sites ranged between 0.51 to 1.39 mg L⁻¹ and 8.7 to 12.8, respectively (Fig. 6, Table 4). Detrital POC dominated the bulk POC pool, comprising 71 to 92% of bulk POC on average. The remaining fractions, 8.3 to 28.6%, were accounted for by organic carbon (OC) that originated from phytoplankton. Mean δ¹³C-detritus and δ¹³C-phytoplankton values followed a salinity gradient, with lowest values at the freshest sites and highest values at more marine sites. Mean bulk POC, POM C:N ratios, and detrital POC contributions were all highest at low to mid-salinity sites (PO-657 to PO-6) and declined across the transect seaward.

Between 2007 and 2016, mean annual bulk POC concentrations ranged between 0.44 to 0.89 mg L⁻¹, and bulk POM C:N ratios averaged 7.7 to 9.6 across all sites (Table 4). Relative to data available from the 1990 to 1996 period, annual bulk POM C:N ratios declined, on average, by 12 to 27%. Annually, mean detrital POC contributions comprised around 54 to 84% of the modern bulk POC pool, with phytoplankton OC contributions increasing in relative importance compared to 1990 to 1996. While phytoplankton OC became a larger component of the bulk POC

Table 1 WRTDS model results showing the mean and standard deviation of TSS concentrations and fluxes in the Sacramento River at Freeport (USGS Station 11447650) through time

	Discharge (cfs)	TSS (mg L ⁻¹)	Flow normalized TSS (mg L ⁻¹)	TSS Flux (Gg yr ⁻¹)	Flow normalized TSS Flux (Gg yr ⁻¹)
1957 to 1965	21,170±7390	79.4±25.4	86.8±6.3	2400±1600	2880±190
1966 to 1975	27,740±7900	72.7±15.8	60.6±5.0	2530±1220	1930±200
1976 to 1985	24,380±12400	53.5±19.3	51.4±7.2	1840±1450	1670±210
1986 to 1995	18,280±9000	36.5±17.7	50.7±3.9	1110±1160	1830±190
1996 to 2005	26,020±7140	49.7±12.6	43.6±2.6	1770±860	1490±80
2006 to 2020	20,280±9940	34.8±15.2	38.4±4.8	1030±1020	1230±120

Fig. 3 Monthly TSS time series data for sites (C3/3A, D4, D8, D7, D6, and D41) from the California Department of Water Resources Interagency Ecological Program's Environmental Monitoring Program (DWR IEP EMP)



pool, in absolute terms, the change was driven by declines in detrital components as phytoplankton OC only changed slightly over this period. Detrital POM C:N ratios declined

substantially as well, with declines greatest (up to 37%) at sites closest to the Delta and its confluence with Suisun Bay.

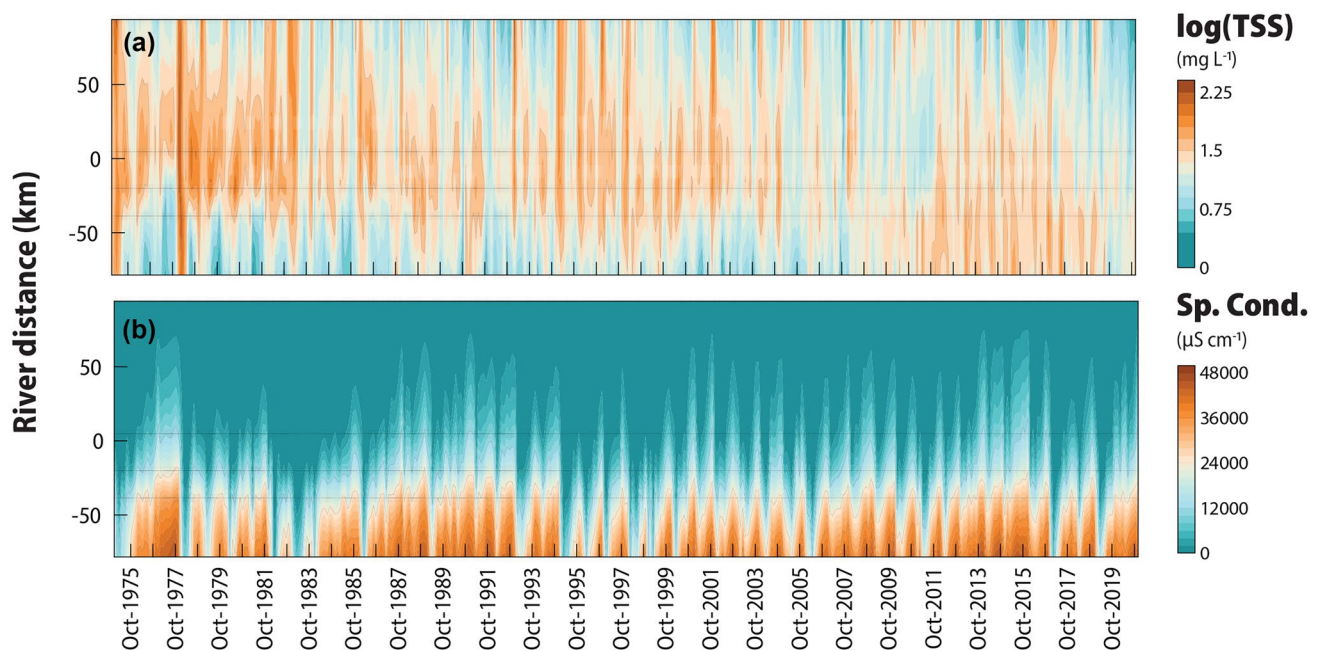


Fig. 4 Contour plots of (a) TSS and (b) specific conductance (Sp. Cond.) for sites (C3/3A, D4, D8, D6, and D41) from the California Department of Water Resources Interagency Ecological Program's Environmental

Monitoring Program (DWR IEP EMP). Site locations are indicated by semi-transparent lines on each plot, with the y-axis minimum starting (negative) at site D41 and ending (positive) with Site C3/3A

Discussion

TSS Shifts in the Estuary

Suspended sediment dynamics in the SF Bay and Delta have changed measurably through time and space (Barnard et al. 2013). Between 1957 and 2020, annual TSS fluxes and annual flow normalized TSS fluxes in the Sacramento River, the major freshwater input to the Delta and downstream SF Bay, saw 56% reductions (Table 1). These reductions are in line with previous work that indicated a 50% decline in sediment supply from the Sacramento River from 1957 to 2001 (Wright and Schoellhamer 2004). Natural variability in flow could not account for the large reductions in TSS concentrations as evidenced by mean annual flow normalized TSS concentrations, which have steadily declined, from $86.8 \pm 6.3 \text{ mg L}^{-1}$ to $38.4 \pm 4.8 \text{ mg L}^{-1}$, since records began in the late 1950s. Declines in TSS in the eastern regions of the SFE and in the Delta are not surprising given recent studies, which show decreases in both sediment supply from the Delta's large rivers and in the overall pool of erodible sediment in the SF Bay (Jaffe et al. 1998; Wright and Schoellhamer 2004).

Historically, sediment pulses associated with hydraulic mining in the mid-1800s to early 1900s helped build up the erodible sediment pool by increasing sediment volume by over 300 million cubic meters between 1856 and 1922 (Ganju et al. 2008; Jaffe et al. 1998). The SF Bay region

broadly changed from net accretional to net erosional likely between 1950 and 1980 as mining was largely phased out and new State Water Projects for flow diversions were implemented (Jaffe et al. 1998). More recent work further suggests that the SF Bay bed sediment pool has been exhausted, driving abrupt declines in modern SFE TSS concentrations and sedimentation rates (Jaffe et al. 1998; Schoellhamer 2011). Schoellhamer (2011) calculated declines of roughly 27 to 53% in TSS concentrations in the SF Bay between the 1990s and early 2000s. Our results suggest declines of 14 to 35% when binned across the same time periods at comparable sites (D4, D6, and D41) (Table S1). While estimates from D4 and D6 were relatively similar, site D41 showed large differences in the magnitude of change (14 versus 53%). The discrepancy in the magnitude of change at D41 may be a result of differences in site location, sampling depth, and data density, as our study uses roughly monthly data collected from the near surface (rather than 15-min resolution at mid-depth) and is in an upstream portion of the main channel that is shallower. The abrupt declines are thought to be from extreme precipitation events during select El Niño water years (1983, 1997, 1998, 2006), which helped flush the remaining erodible sediment pool downstream (Hestir et al. 2013; Schoellhamer et al. 2018). The washout and insufficient replenishment of bed sediment have converted the SF Bay region of the SFE from transport to supply regulation (Schoellhamer 2011). This crossover increases system

Table 2 Mean (and standard deviation, 'SD') TSS concentrations at DWR IEP monitoring sites. Data was binned into four generally decadal periods. Annual averages were taken as the mean of the seasonal values

Station	Season		TSS (mg L ⁻¹)				
			1975 to 1985	1986 to 1995	1996 to 2005	2006 to 2020	
C3/3A	Fall	Mean	25.7	9.5	21.4	13.1	
		SD	38.9	12.1	36.7	25.3	
	Winter	Mean	46.8	44.9	39.8	30.4	
		SD	49.0	54.4	29.1	36.0	
	Spring	Mean	22.9	14.4	20.8	18.7	
		SD	24.6	13.1	19.6	13.0	
	Summer	Mean	14.8	12.8	11.7	12.5	
		SD	6.1	6.2	3.5	8.1	
	Annual	Mean	27.5	20.4	23.4	18.7	
		SD	13.6	16.4	11.8	8.3	
	D4	Fall	Mean	40.3	20.6	36.3	20.5
			SD	25.3	11.7	51.0	17.3
Winter		Mean	55.2	36.6	39.8	24.1	
		SD	87.9	27.7	55.4	14.1	
Spring		Mean	44.9	32.2	30.3	23.4	
		SD	22.6	12.2	13.8	14.9	
Summer		Mean	46.9	34.3	29.4	21.3	
		SD	23.6	17.7	11.0	9.5	
Annual		Mean	46.8	30.9	34.0	22.3	
		SD	6.2	7.1	5.0	1.7	
D8		Fall	Mean	42.1	24.6	40.1	24.4
			SD	24.2	16.1	38.3	12.7
	Winter	Mean	47.1	37.2	34.9	24.8	
		SD	63.5	24.0	19.9	12.8	
	Spring	Mean	48.9	34.4	38.4	24.4	
		SD	25.7	16.9	22.1	12.5	
	Summer	Mean	46.7	37.0	34.2	19.1	
		SD	30.0	18.8	16.3	7.2	
	Annual	Mean	46.2	33.3	36.9	23.2	
		SD	2.9	6.0	2.8	2.7	
	D7	Fall	Mean	71.5	38.4	39.8	37.4
			SD	51.2	23.1	20.8	23.2
Winter		Mean	50.8	43.7	52.2	45.1	
		SD	37.6	36.6	39.3	26.8	
Spring		Mean	67.9	44.2	49.3	49.6	
		SD	38.7	19.8	26.2	27.8	
Summer		Mean	76.8	65.8	63.7	50.0	
		SD	55.0	40.9	42.5	40.8	
Annual		Mean	66.8	48.0	51.2	45.5	
		SD	11.3	12.1	9.9	5.9	
D6		Fall	Mean	20.3	18.4	26.6	23.0
			SD	15.1	10.9	18.2	9.2
	Winter	Mean	37.7	27.0	33.9	30.5	
		SD	36.0	15.1	26.2	19.9	
	Spring	Mean	26.6	22.0	25.4	32.5	
		SD	23.3	10.4	13.0	16.0	
	Summer	Mean	15.0	23.6	21.1	29.7	
		SD	10.1	13.3	6.6	16.5	
	Annual	Mean	24.9	22.8	26.7	28.9	
		SD	9.8	3.6	5.3	4.1	

Table 2 (continued)

Station	Season		TSS (mg L ⁻¹)			
			1975 to 1985	1986 to 1995	1996 to 2005	2006 to 2020
D41	Fall	Mean	10.2	12.8	12.4	22.8
		SD	4.7	10.1	8.8	13.5
	Winter	Mean	17.7	13.9	15.5	21.9
		SD	13.7	9.1	10.1	11.5
	Spring	Mean	8.7	14.1	11.7	26.4
		SD	7.7	8.6	6.5	16.0
	Summer	Mean	7.8	13.2	12.1	27.1
		SD	3.9	9.8	8.5	18.2
	Annual	Mean	11.1	13.5	12.9	24.5
		SD	4.5	0.6	1.8	2.6

reliance on upstream inputs from rivers. The upstream portion of the SFE, the Delta, is still considered net depositional, as this area is the first large-scale depositional environment major rivers encounter in the region; thus, sediment supply from the rivers influences the magnitude of the rate of deposition in this area only (Wright and Schoellhamer 2005).

This system switchover in the SF Bay region likely explains why mid-salinity sites (D4, D7, and D8) downstream of the Delta also recorded widespread reductions in TSS concentrations, on the order of 32 to 52%, with declines greatest in summer months but still pronounced through all seasons. The increased reliance on upstream TSS coupled with long-term reductions in riverine TSS inputs through time ultimately act together to limit material available for re-suspension, transport, and cycling internal to the system. Additionally, since function is governed by supply, there is a greater dependency on water year variability. In the past, shortcomings in riverine TSS exports during dry years could likely be masked by bed supply and transport regulated. The widespread expansion of invasive submerged aquatic vegetation (SAV) in the Delta may also be contributing to changes in Delta TSS concentrations, as SAV has been shown to trap

sediment and reduce turbidity (Greenfield et al. 2007; Hestir et al. 2016).

While over long-time scales, many parts of SF Bay are net erosional, dry water years with low freshwater discharge can favor gravitational circulation and help shift the sediment balance towards net deposition. Landward TSS fluxes dominated low discharge years between 2002 and 2016 at Benicia Bridge in Suisun Bay; this allowed for net deposition to occur as sediment was imported from both the landward and seaward boundaries (Schoellhamer et al. 2018).

The spatial context of TSS inputs has also shifted as the major riverine sediment sources to the SFE migrated

Table 3 Sen’s slope values from annualized Mann–Kendall tests for specific conductivity (Sp. Cond.), TSS, and Chl. a at DWR IEP sites. Significance at $p < 0.10$ is indicated by an asterisk (*) and $p < 0.05$ is indicated by double asterisks (**)

Site	Sp. Cond. ($\mu\text{s cm}^{-1} \text{yr}^{-1}$)	TSS ($\text{mg L}^{-1} \text{yr}^{-1}$)	Chl. a ($\mu\text{g L}^{-1} \text{yr}^{-1}$)
C3/3A	-0.10	-0.24*	0.00
D4	42	-0.52**	-0.06**
D8	27	-0.57**	-0.07**
D7	72	-0.44**	-0.07**
D6	16	0.24**	-0.04**
D41	112	0.44**	-0.02**

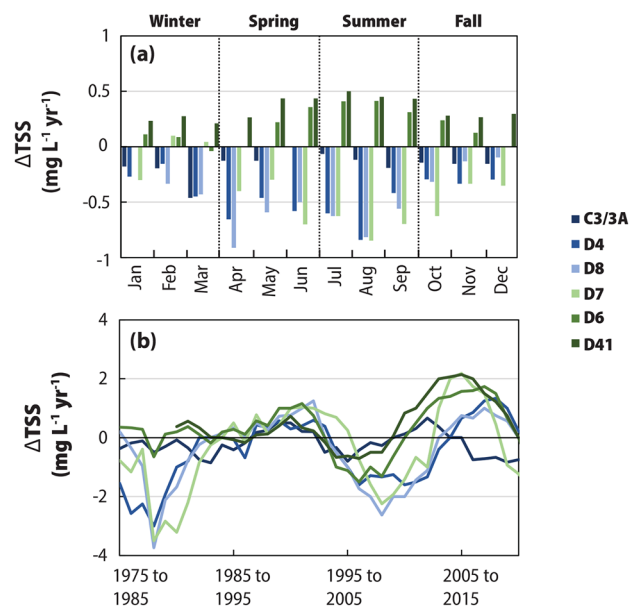
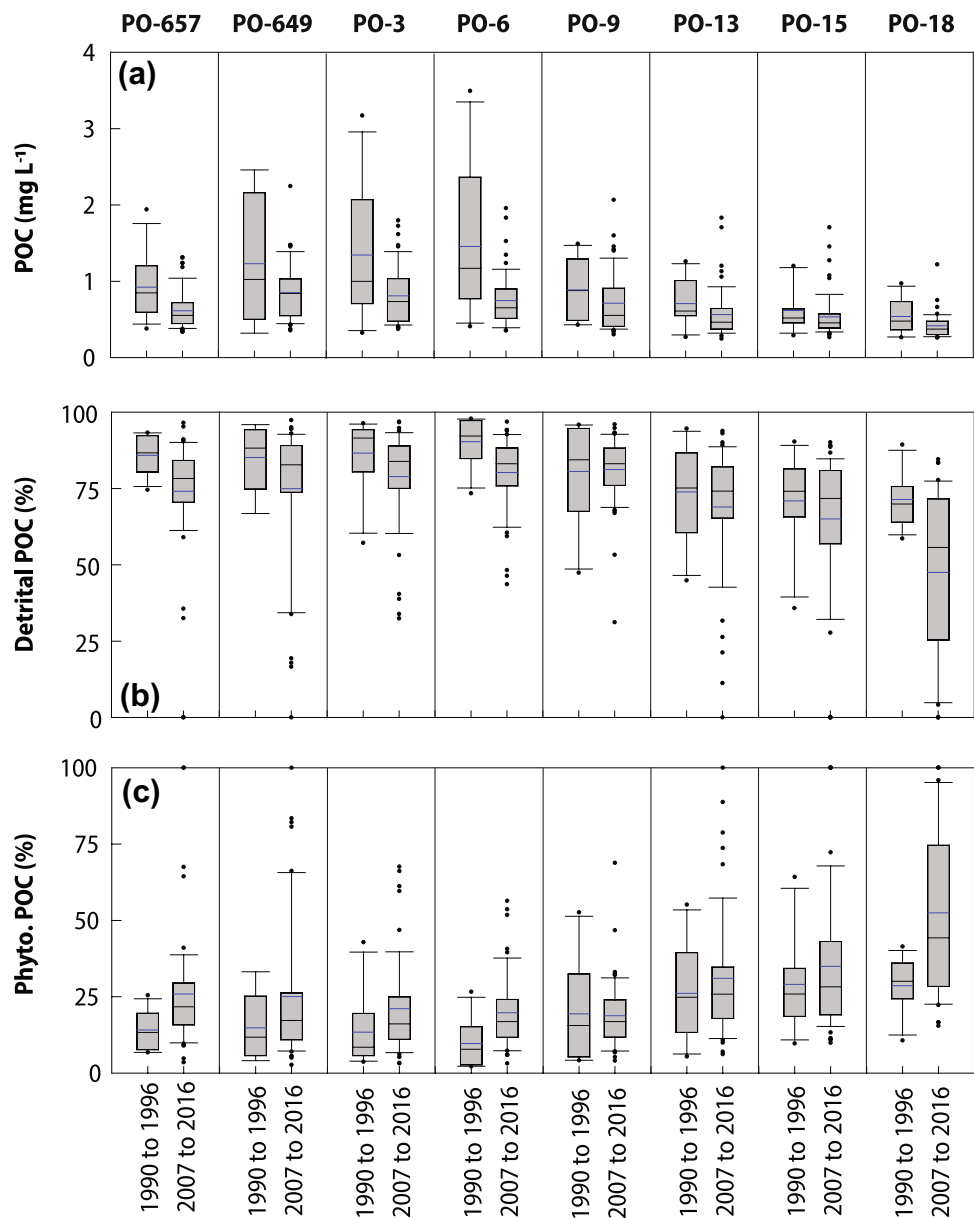


Fig. 5 Long-term changes in total suspended sediment (ΔTSS) concentrations by **a** month, and **b** 10-year rolling windows of change. Data from the California Department of Water Resources Interagency Ecological Program’s Environmental Monitoring Program (DWR IEP EMP)

Fig. 6 Box and whisker plots of **a** POC concentrations, **b** detrital POC as a percentage of the total POC pool, and **c** phytoplankton POC as a percentage of the total POC pool. Boxes represent the bounds of the middle quartiles, and black lines represent median values. Blue lines show mean values. Whiskers show the bounds of the outer quartiles (5th and 95th) of the data



seaward. SF Bay tributaries dominated sediment supply to the SFE in 10 out of 16 years analyzed between water years 1995 to 2010, and although these tributaries contribute just 7% of freshwater discharge, they accounted for over 60% of TSS inputs to the SF Bay (McKee et al. 2013). Further, a majority of TSS enters the SFE during the winter rainy season (Wright and Schoellhamer 2005), when hydrologic conditions shift to include flow paths that facilitate increased material transport and supply from terrestrial sources. Results from this study show substantial long-term declines of 52% (72 mg L⁻¹) and 56% (3560 Gg yr⁻¹) in upstream Sacramento River flow normalized TSS concentrations and fluxes during the winter, respectively (Fig. S1). Mean averages for fresh and brackish water sites across seasons and binned decades similarly show that TSS concentrations

declined substantially during these time periods. Such declines provide important temporal and spatial context for observed changes in the POM pool. As TSS inputs during the winter have declined across the most freshwater-influenced sites, it follows that autochthonous POM supply has also been impacted as these sources are mobilized through many of the same runoff generation mechanisms.

In contrast, at the North Bay sites (D6, D41), TSS concentrations have increased since the IEP EMP monitoring program began in 1975 to 1980, though the period of increase was relatively recent, during the last two decades, and greatest in the spring and summer months. Seasonal cycles in sediment dynamics are common in San Pablo Bay (Krone 1979; Schoellhamer et al. 2008). Like Suisun Bay, a large fraction of sediment enters during periods of high

Table 4 Mean historical and modern values for parameters by site and season. Data was filtered to exclude any samples with Chl. a concentrations above 10 ug L⁻¹, which was assumed to represent periods where phytoplankton dominated the bulk POC pool during bloom events. Annual averages were taken as the mean of the seasonal values

Salinity	TSS (mg L ⁻¹)			POM (C:N) _m			POC (mg L ⁻¹)			Detrital POC (C:N) _m			Detrital POC (mg L ⁻¹)			δ ¹³ C-Detritus (‰)			Phytoplankton POC (mg L ⁻¹)			δ ¹³ C-Phytoplankton (‰)					
	1990 to 1996	2007 to 2016	1990 to 2016	1990 to 1996	2007 to 2016	1990 to 2016	1990 to 1996	2007 to 2016	1990 to 2016	1990 to 1996	2007 to 2016	1990 to 1996	2007 to 2016	1990 to 1996	2007 to 2016	1990 to 1996	2007 to 2016	1990 to 1996	2007 to 2016	1990 to 1996	2007 to 2016	1990 to 1996	2007 to 2016	1990 to 1996	2007 to 2016		
Fall																											
PO-657	0.2	0.6	16.8	21.1	13.0	9.2	0.58	0.59	14.5	10.1	0.49	0.42	-27.9	-27.4	0.10	0.11	-30.0	-29.9									
PO-649	2.6	3.5	21.9	25.8	11.6	9.9	0.75	0.68	12.9	12.0	0.67	0.55	-28.9	-28.3	0.09	0.13	-29.3	-29.2									
PO-3	4.7	6.1	15.5	21.2	11.9	9.4	0.52	0.59	13.4	10.5	0.39	0.41	-27.9	-27.4	0.13	0.12	-28.5	-28.4									
PO-6	10.0	12.1	20.3	17.3	13.5	9.1	0.64	0.52	14.9	10.1	0.54	0.41	-27.3	-26.9	0.11	0.11	-26.8	-26.8									
PO-9	17.7	19.1	22.2	14.4	9.5	8.6	0.47	0.47	10.1	9.3	0.39	0.37	-27.4	-26.4	0.08	0.10	-25.2	-24.9									
PO-13	24.3	26.6	18.9	10.3	8.6	7.6	0.34	0.40	9.5	9.3	0.25	0.24	-27.7	-27.9	0.09	0.16	-22.9	-22.9									
PO-15	27.3	27.3	13.1	11.4	10.7	7.7	0.39	0.42	12.6	9.1	0.28	0.25	-28.1	-25.8	0.11	0.18	-22.5	-22.7									
PO-18	30.6	30.9	10.4	8.6	9.2	7.7	0.32	0.37	10.7	9.6	0.21	0.19	-25.2	-22.4	0.10	0.17	-21.6	-21.4									
Winter																											
PO-657	0.1	0.2	100.4	35.7	12.5	9.6	1.49	0.86	13.0	10.2	1.39	0.73	-26.2	-27.0	0.11	0.12	-30.4	-30.3									
PO-649	0.1	1.0	111.7	48.1	15.0	10.2	2.41	1.08	15.4	10.5	2.30	0.98	-26.3	-26.7	0.12	0.09	-30.4	-30.1									
PO-3	1.1	2.4	70.0	45.0	12.9	10.5	2.05	1.02	13.2	11.1	1.96	0.91	-26.2	-26.5	0.09	0.10	-30.0	-29.7									
PO-6	4.3	6.0	45.7	43.6	14.3	10.1	1.44	1.00	14.9	10.7	1.38	0.87	-26.3	-26.1	0.06	0.12	-29.1	-28.6									
PO-9	10.3	12.0	42.1	35.8	13.1	9.9	1.05	0.86	14.2	10.6	0.96	0.74	-26.1	-26.5	0.08	0.12	-27.3	-26.8									
PO-13	20.0	21.9	14.7	17.3	9.6	8.7	0.64	0.52	10.6	9.4	0.51	0.41	-25.3	-25.6	0.14	0.11	-24.3	-23.7									
PO-15	22.2	22.5	14.2	14.8	10.1	9.8	0.50	0.48	11.6	13.8	0.38	0.35	-26.6	-25.0	0.12	0.12	-23.7	-23.6									
PO-18	29.4	29.2	13.1	14.6	10.4	8.6	0.51	0.48	11.5	10.8	0.43	0.30	-25.6	-23.9	0.08	0.20	-21.5	-21.3									
Spring																											
PO-657	0.1	0.1	19.6	23.3	9.9	8.8	0.70	0.63	10.5	9.7	0.58	0.47	-27.6	-27.2	0.12	0.16	-30.3	-30.3									
PO-649	0.1	1.5	28.9	47.4	11.2	9.5	0.88	1.07	11.8	10.6	0.76	0.87	-27.4	-27.0	0.12	0.20	-30.3	-29.9									
PO-3	0.3	3.0	45.0	46.1	11.1	9.1	1.27	1.04	11.3	10.0	1.11	0.86	-27.0	-26.3	0.16	0.18	-30.3	-29.4									
PO-6	1.7	7.8	70.4	35.4	11.1	8.8	1.89	0.85	11.4	9.4	1.75	0.71	-26.5	-26.5	0.14	0.14	-29.4	-27.9									
PO-9	10.3	13.7	34.8	42.8	10.0	8.6	1.01	0.98	11.7	9.1	0.71	0.85	-27.7	-26.1	0.30	0.13	-27.7	-26.0									
PO-13	18.8	21.9	25.6	35.2	9.1	8.2	0.80	0.85	11.0	9.0	0.50	0.67	-26.9	-26.5	0.30	0.18	-23.0	-23.4									
PO-15	21.1	23.1	30.7	31.0	8.8	8.0	0.83	0.77	10.4	8.8	0.50	0.57	-26.4	-26.0	0.33	0.20	-22.9	-23.0									
PO-18	29.5	28.4	10.5	18.3	8.1	7.6	0.67	0.54	9.2	11.5	0.46	0.26	-25.4	-29.2	0.21	0.28	-20.8	-21.4									
Summer																											
PO-657	0.1	0.1	15.2	14.7	13.6	8.7	0.83	0.48	14.9	9.3	0.73	0.37	-27.7	-27.9	0.11	0.11	-29.2	-29.2									
PO-649	0.2	1.6	23.7	28.5	12.7	8.9	0.86	0.73	13.9	10.2	0.72	0.59	-26.8	-26.3	0.14	0.16	-29.1	-28.8									
PO-3	2.0	3.5	53.5	26.8	14.2	9.4	1.27	0.69	14.9	10.1	1.15	0.57	-25.6	-26.8	0.11	0.13	-28.3	-28.2									
PO-6	5.8	9.1	57.7	25.8	12.2	9.2	1.58	0.68	12.6	9.9	1.50	0.56	-26.0	-26.0	0.08	0.12	-26.7	-26.7									

Table 4 (continued)

	Salinity			TSS (mg L ⁻¹)			POM (C:N) _m			POC (mg L ⁻¹)			Detrital POC (C:N) _m			Detrital POC (mg L ⁻¹)			δ ¹³ C-Detritus (‰)			Phytoplankton POC (mg L ⁻¹)			δ ¹³ C-Phytoplankton (‰)				
	1990 to 1996	2007 to 2016	1990 to 2016	1990 to 1996	2007 to 2016	1990 to 2016	1990 to 1996	2007 to 2016	1990 to 2016	1990 to 1996	2007 to 2016	1990 to 1996	2007 to 2016	1990 to 1996	2007 to 2016	1990 to 1996	2007 to 2016	1990 to 1996	2007 to 2016	1990 to 1996	2007 to 2016	1990 to 1996	2007 to 2016	1990 to 1996	2007 to 2016	1990 to 2016	2007 to 2016		
PO-9	16.5	16.4	33.0	25.2	8.9	10.6	8.9	0.92	0.67	11.7	9.7	0.82	0.55	-28.0	-25.7	0.10	0.11	-24.0	-24.7										
PO-13	23.1	25.8	21.2	19.4	9.9	7.7	7.7	0.90	0.56	10.9	8.3	0.73	0.42	-27.4	-25.4	0.16	0.14	-22.0	-22.1										
PO-15	24.9	27.0	17.7	19.3	8.5	7.7	7.7	0.71	0.56	9.2	8.4	0.55	0.42	-25.5	-25.3	0.16	0.14	-21.4	-21.8										
PO-18	30.5	31.4	8.5	8.4	7.1	7.1	7.1	0.55	0.36	7.6	9.6	0.37	0.19	-23.9	-23.3	0.17	0.18	-20.7	-20.9										
Annual																													
PO-657	0.1	0.2	38.0	23.7	12.3	9.1	9.1	0.90	0.64	13.2	9.8	0.79	0.50	-27.4	-27.4	0.11	0.13	-30.0	-29.9										
PO-649	0.7	1.9	46.5	37.5	12.6	9.6	9.6	1.23	0.89	13.5	10.8	1.11	0.75	-27.4	-27.1	0.12	0.14	-29.8	-29.5										
PO-3	2.0	3.8	46.0	34.8	12.5	9.6	9.6	1.28	0.84	13.2	10.4	1.15	0.69	-26.7	-26.8	0.12	0.13	-29.3	-28.9										
PO-6	5.5	8.8	48.5	30.5	12.8	9.3	9.3	1.39	0.76	13.5	10.0	1.29	0.64	-26.7	-26.4	0.10	0.12	-28.4	-27.5										
PO-9	13.7	15.3	33.0	29.5	10.8	9.0	9.0	0.86	0.74	11.9	9.7	0.72	0.63	-27.3	-26.2	0.14	0.11	-26.0	-25.6										
PO-13	21.5	24.1	20.1	20.5	9.3	8.1	8.1	0.67	0.58	10.5	9.0	0.50	0.43	-26.8	-26.3	0.17	0.15	-23.1	-23.0										
PO-15	23.8	25.0	18.9	19.1	9.5	8.3	8.3	0.61	0.56	10.9	10.0	0.43	0.40	-26.7	-25.5	0.18	0.16	-22.6	-22.8										
PO-18	30.0	30.0	10.6	12.5	8.7	7.7	7.7	0.51	0.44	9.7	10.4	0.37	0.23	-25.0	-24.7	0.14	0.21	-21.2	-21.3										

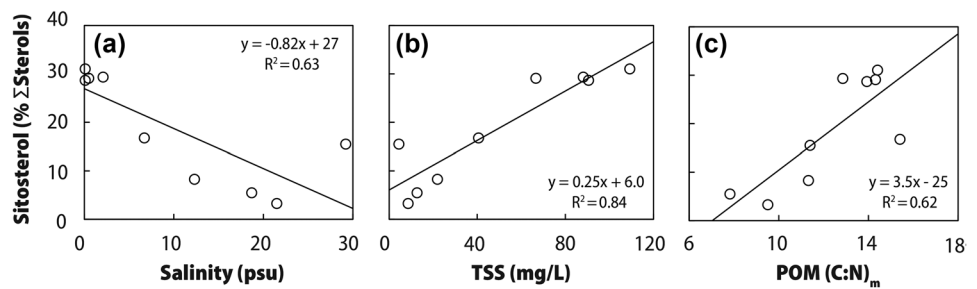
winter and spring freshwater flow, and wind-driven waves help resuspend this material for tidal transport later, during the spring and summer months. While wind waves typically help drive summer TSS increases in these regions, recent work has shown that wind speed is declining in some areas of the SF Bay (Bever et al. 2018), and the persistence of the increase through seasons suggests wind-wave resuspension is likely not the main driver of change. The recent rise may instead be a function of changes in sediment properties and balances in the different embayments, the propagation of long-term upstream change in TSS exports moving through the system, and/or longer periods of influence, like climate cycles, that can broadly influence regional supply. Recent work suggests that San Pablo Bay is net erosional, though, at smaller spatial scales, some areas appear to be accreting (Jaffe et al. 2007). Eleven of the fifteen 2006–2020 water years were also below normal, dry, or critical, and the start of the steeper increase appeared to initiate close to a dry water year (2007) and two back-to-back critical water years (2008 to 2009) (Fig. S2). In the South Bay, increases in TSS can be shoal sourced during dry water years from changes in cross-channel density gradients (Livsey et al. 2021). Past work has also found that large-scale climate systems, like the Pacific Decadal Oscillation (PDO), can control estuary dynamics (Cloern et al. 2010). The recent rise at these sites appears to be shifting downward towards the end of the records, starting around water year 2018 (following the wet water year of 2017). More work is needed to understand the causal factors driving both the relatively rapid increase and subsequent decline in TSS at these locations (Figs. 3 and 5b).

Changes in Estuarine POM Quality and Quantity

The reductions in TSS at low to mid-salinity sites, which typically demarcate the turbidity maximum zone, are also largely reflected in changes observed within the POM pool. Bulk and detrital POC concentrations and C:N ratios generally declined from historic to modern times, and the declines were often greatest at eastern low- and mid-salinity regions of the SFE. Ranges in δ¹³C-POC and δ¹³C-detritus values did not show any substantial changes. ¹³C/¹²C of DIC drives trends in bulk δ¹³C-POC values in this system as spatial gradients in DIC sources incorporated into primary producers change as the system moves from freshwater to marine waters. This spatial gradient is so large that it generally masks any ¹³C/¹²C signatures of specific primary producer groups in spatial comparisons apart from C₄ plants (e.g., grasses), which are frequently isotopically distinct due to small fractionation factors relative to C₃ plants (Deines 1980; Kendall and McDonnell 2012).

Changes to bulk POM C:N ratios can almost exclusively be attributed to shifts in detrital C:N ratios rather than

Fig. 7 Sitosterol (as a percent of total sterol concentrations) versus **a** salinity, **b** TSS, and **c** POM (C:N)_m ratios. Data from Cloern et al. (1993)



changes in phytoplankton abundance, with high C:N material contributions to the system declining over the past three decades (and likely as far as back as the first documented declines in riverine TSS supply beginning in the mid-1900s). Terrestrial plants and soil OM are characterized by high C:N ratios relative to plankton, which typically approach the Redfield ratio (Finlay and Kendall 2007). In this system, past work has shown mean C:N ratios for terrestrial plant species range between ~16 and 40 (Cloern et al. 2002), and this range is consistent with estimates from other large watersheds (Kendall et al. 2001). Soil OM is typically slightly lower in range, between 8 and 15, but can have higher C:N ratios depending on land use and geographic region as soil characteristics (e.g., temperature, OM quantity/quality) influence degradation processes that control C:N values (Kendall et al. 2001).

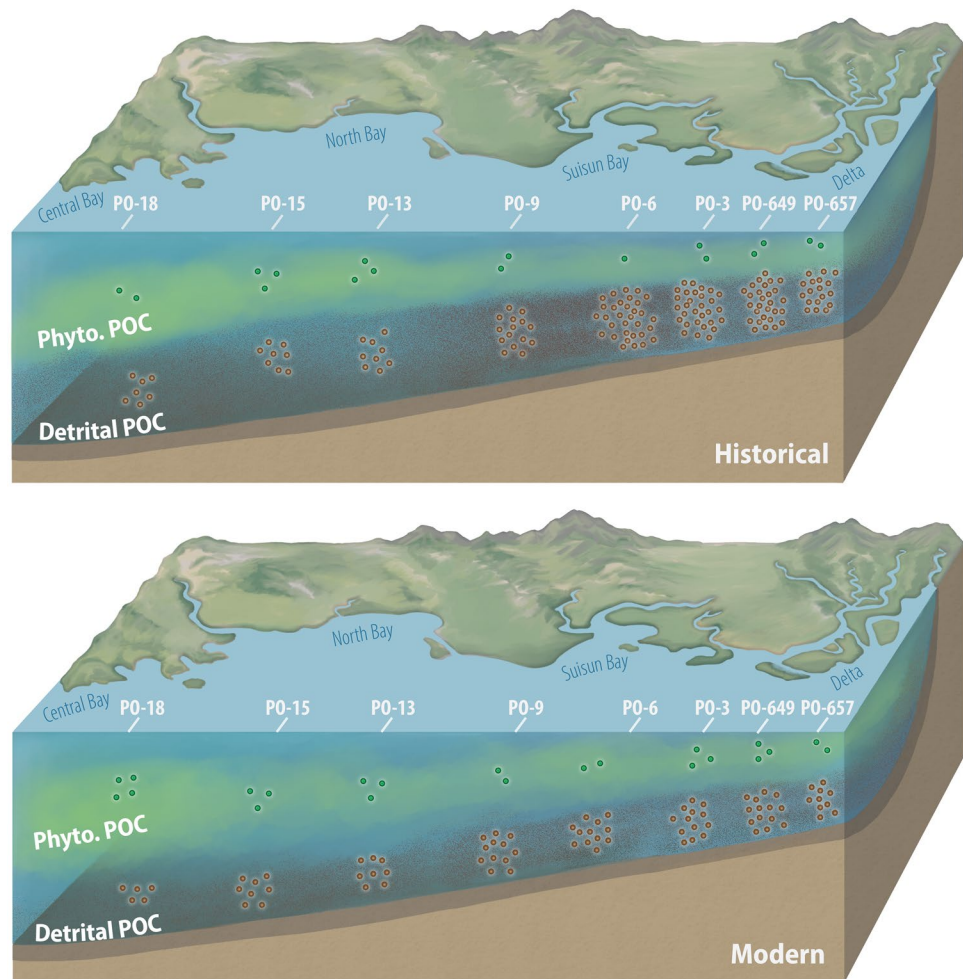
High C:N ratio terrestrial inputs occur predominantly in the rainy season, when flow paths that are capable of moving large soil and plant material are activated by rainfall (Kendall et al. 2001). Results from this study show that riverine TSS concentrations and fluxes are seasonally greatest in the winter and that declines in upstream sediment inputs have also been most substantial during the winters of 1957 to 2020 (Fig. S1). Beyond the washout of hydraulic mining associated TSS (which was predicted to generally cease by the 1950s) (Gilbert 1917), reductions in riverine TSS may also be from increases in upstream reservoir sedimentation and stream bank protection (Wright and Schoellhamer 2004). Sediment deposition from just three reservoirs constructed between 1940 and 1967 in the Sacramento River Watershed can account for the same order of magnitude as the observed decreases in Sacramento River TSS yields (Wright and Schoellhamer 2004). Ultimately, long-term declines in terrestrial material inputs ripple through the system as reduced contributions to suspended and sedimentary pools. The suspended pool directly sees declines in POM C:N ratios. Indirectly, this change in material balance over decades may act to shift the C:N ratio of the resuspended POM pool as well, with cascading effects on downstream POM quality, where resuspended material is likely an important contributor to the POM pool. Canuel et al. (2009) found sediment and TOC accumulation rates generally decreased in cores from the Delta between 1954 and 2005.

The declines also align with historical biomolecular measurements. We revisited snapshot biomolecular data from Cloern et al. (1993) to see if historical sitosterol concentrations, an indicator of vascular plant sources, from the low- to mid-salinity sites corresponded with high POM C:N ratios as Canuel et al. (1995) showed abundant sitosterol concentrations in POM samples collected at low to mid salinity sites (PO-657 to PO-6). While the sample sizes were limited, we found relatively strong positive correlations amongst comparisons of sitosterol (taken as a weight percentage of total sterol concentration) versus salinity ($R^2=0.63$), TSS ($R^2=0.84$), and bulk POM C:N ratios ($R^2=0.62$) (Fig. 7). These correlations support the idea that terrestrial contributions to the bulk POM pool, historically, were greatest at low salinity sites, and consistent with higher bulk POM C:N ratios (which were uncommon in the modern dataset we analyzed).

Building on this, Hernes et al. (2020) observed large declines in modern mean bulk C:N ratios of POM from the north SF Bay. Interestingly, their biomolecular data showed that lignin concentrations in recent POM data did not trend with low salinities, high TSS values, or high POM C:N ratios as expected. As upland terrestrial contributions from the Delta decline, these relationships should start to break down. Additionally, Hernes et al. (2020) POM and biomolecular data show a reversed spatial trend, where spatially averaged carbon-normalized yields of lignin and POM C:N ratios were highest in the more brackish water samples from the north SF Bay (and west of the Delta's large rivers), and they estimate that 13–60% of POC in this region may be wetland derived. This finding could reflect the shift in importance of sediment and related material inputs from large Delta rivers to smaller SF Bay tributaries. Many of the SF Bay's tributaries feed into tidal wetlands, which can modulate and alter OM inputs, so material fluxes through these systems may shift the quality of POM pulsed into the greater bay and lead to spatial discrepancies in more terrestrial proxies of OM.

Other related biogeochemical indices hint at changes to the suspended and sediment pools as well. Bulk sediment OC samples collected in 2006 in the Delta had a mean C:N ratio of 14.6 (Wakeham and Canuel 2016), and more recent

Fig. 8 Conceptual figure showing general changes in POC pools across historical (considered as the 1990 to 1996 datasets) and modern periods of record (2007 to 2016). Each circular marker is roughly equivalent to 0.05 mg-C L^{-1} . Site transects and depth are not to scale and values are intended to be semi-quantitative



data shows sedimentary organic carbon collected from the Sacramento River in 2019 had much lower C:N ratios (~6.8 to 7.7) (Pondell et al. 2020). The widespread growth of invasive aquatic plants may also help to lower bulk C:N ratios in conjunction with declines from terrestrial sources; *Myriophyllum brasiliense* (Parrot's Feather) and *Egeria densa* (Brazilian Waterweed) both have low C:N ratios (Cloern et al. 2002) and have spread significantly throughout the Delta's waterways since their indeliberate introduction (Ta et al. 2017). Management of invasive SAV in the Delta includes mechanical shredding, which may help artificially generate in situ low C:N ratio POM from these sources as well (Greenfield et al. 2007).

Taken together, these results suggest that terrestrial POM contributions to the SFE are now lower than historical values from the 1990s (and likely earlier, into the mid to late 1900s, based on the long-term declines in upstream TSS supply) (Fig. 8). The partial loss of terrestrial OM may have widespread metabolic consequences for the estuarine food web as terrestrial OM is used for microbial respiration as documented in other rivers (Ward et al. 2017). The breakdown

of terrestrial POM is often facilitated by changes in estuarine ecosystem gradients, where new molecules (e.g., algal-derived) may help prime material transported from upstream for microbial processing (Bianchi et al. 2015; Bonin et al. 2019). There is also evidence that the refractory plant OM is selectively consumed by copepods in the SFE (Harfmann et al. 2019). Changes to estuarine biogeochemistry may not be limited to fresh and brackish water regions. For example, shifts in OM supply can have consequences for the long-term burial of OM. In addition, with the loss of higher C:N material and the erodible sediment pool, more landward freshwater portions of the estuary may more closely follow marine biogeochemical pathways. Typically, in estuaries, POM bordering the seaward side starts to compositionally reflect marine-dominant sources (e.g., phytoplankton, zooplankton pellets, bacteria) and biogeochemical pathways (e.g., degradation), with low C:N ratios relative to terrestrial sources (Allredge 1998; Canuel and Hardison 2016; Hollibaugh et al. 2000). Such chronic perturbations in dominant POM sources across the SFE may play a role in the ongoing and widespread ecosystem change in this system.

Conclusions

We synthesized existing long-term monitoring program TSS data together with synoptic POM composition and stable isotope data to examine how TSS and related POC dynamics have evolved in the San Francisco Bay and Sacramento-San Joaquin Delta in central California over the past ~45 years. TSS data was used to contextualize spatial and temporal changes seen in the synoptic POC dataset. We found large declines, on average, of 32 to 56% in TSS concentrations at fresh and brackish water sites. At the same time, the sources of POM, as indicated by declines in bulk and detrital C:N ratios, have shifted at these eastern SFE sites, by 23 to 27%, on average (and by 12 to 27% across all sites). Based on the synoptic elemental ratio data and the corresponding changes in TSS discussed above, the declines in bulk and detrital C:N ratios appear to be driven by a loss of material that is mostly terrestrial in origin. This material loss may have implications for both suspended and sedimentary OM pools, both of which could impact food web dynamics across the estuary. Our experience using existing monitoring datasets demonstrates that even incomplete or irregularly spaced datasets can provide meaningful new insight, especially when leveraged together with other existing data. More broadly, this work highlights how upstream human impacts can ripple through estuarine systems with long-term consequences for OM sources and transport.

Supplementary Information The online version contains supplementary material available at <https://doi.org/10.1007/s12237-022-01160-z>.

Acknowledgements The authors thank Carol Kendall for her dedication and effort to spearhead the POM data collected and used in this study, and others who have likewise advocated for maintaining long-term monitoring programs in the SFE. We also thank the Delta Stewardship Council and California Sea Grant for funding this work, under R/SF-100. We thank our two reviewers for useful feedback and suggestions. We thank Amanda Riley for her illustration help. Any use of trade, firm, or product names is for descriptive purposes only and does not imply endorsement by the U.S. Government.

Data Availability The Polaris Stable Isotope and Elemental Ratio data are available through HydroShare via the Consortium of Universities for the Advancement of Hydrologic Science, Inc. (CUAHSI): <http://www.hydroshare.org/resource/86b6ed28efc64381b2f84adc5b2e4b63>. Other data sources are publicly available as described and linked in the Data Sources section.

Open Access This article is licensed under a Creative Commons Attribution 4.0 International License, which permits use, sharing, adaptation, distribution and reproduction in any medium or format, as long as you give appropriate credit to the original author(s) and the source, provide a link to the Creative Commons licence, and indicate if changes were made. The images or other third party material in this article are included in the article's Creative Commons licence, unless indicated otherwise in a credit line to the material. If material is not included in the article's Creative Commons licence and your intended use is not permitted by statutory regulation or exceeds the permitted use, you will need to obtain permission directly from the copyright holder. To view a copy of this licence, visit <http://creativecommons.org/licenses/by/4.0/>.

References

- Allredge, A. 1998. The carbon, nitrogen and mass content of marine snow as a function of aggregate size. *Deep Sea Research Part I: Oceanographic Research Papers* 45 (4–5): 529–541.
- Barnard, P.L., D.H. Schoellhamer, B.E. Jaffe, and L.J. McKee. 2013. Sediment transport in the San Francisco Bay coastal system: An overview. *Marine Geology* 345: 3–17.
- Bever, A.J., M.L. MacWilliams, and D.K. Fullerton. 2018. Influence of an observed decadal decline in wind speed on turbidity in the San Francisco Estuary. *Estuaries and Coasts* 41 (7): 1943–1967.
- Bianchi, T.S., D.C. Thornton, S.A. Yvon-Lewis, G.M. King, T.I. Eglinton, M.R. Shields, N.D. Ward, and J. Curtis. 2015. Positive priming of terrestrially derived dissolved organic matter in a freshwater microcosm system. *Geophysical Research Letters* 42 (13): 5460–5467.
- Bonin, P., A.-H. Prime, M.-A. Galeron, S. Guasco, and J.-F. Rontani. 2019. Enhanced biotic degradation of terrestrial POM in an estuarine salinity gradient: Interactive effects of organic matter pools and changes of bacterial communities. *Aquatic Microbial Ecology* 83 (2): 147–159.
- Caffrey, J.M. 2004. Factors controlling net ecosystem metabolism in US estuaries. *Estuaries* 27 (1): 90–101.
- Canuel, E.A., J.E. Cloern, D.B. Ringelberg, J.B. Guckert, and G.H. Rau. 1995. Molecular and isotopic tracers used to examine sources of organic matter and its incorporation into the food webs of San Francisco Bay. *Limnology and Oceanography* 40 (1): 67–81.
- Canuel, E.A., and A.K. Hardison. 2016. Sources, ages, and alteration of organic matter in estuaries. *Annual Review of Marine Science* 8: 409–434.
- Canuel, E.A., E.J. Lerberg, R.M. Dickhut, S.A. Kuehl, T.S. Bianchi, and S.G. Wakeham. 2009. Changes in sediment and organic carbon accumulation in a highly-disturbed ecosystem: The Sacramento-San Joaquin River Delta (California, USA). *Marine Pollution Bulletin* 59 (4–7): 154–163.
- Cloern, J.E. 2019. Patterns, pace, and processes of water-quality variability in a long-studied estuary. *Limnology and Oceanography* 64 (S1): S192–S208.
- Cloern, J.E., P.C. Abreu, J. Carstensen, L. Chauvaud, R. Elmgren, J. Grall, H. Greening, J.O.R. Johansson, M. Kahru, and E.T. Sherwood. 2016. Human activities and climate variability drive fast-paced change across the world's estuarine-coastal ecosystems. *Global Change Biology* 22 (2): 513–529.
- Cloern, J.E., E.A. Canuel, and D. Harris. 2002. Stable carbon and nitrogen isotope composition of aquatic and terrestrial plants of the San Francisco Bay estuarine system. *Limnology and Oceanography* 47 (3): 713–729.
- Cloern, J.E., E.A. Canuel, and S.M. Wienke. 1993. Particulate organic matter in the San Francisco Bay Estuary, California: chemical indicators of its origin and assimilation into the benthic food web. *US Geological Survey*.
- Cloern, J.E., S. Foster, and A. Kleckner. 2014. Phytoplankton primary production in the world's estuarine-coastal ecosystems. *Biogeosciences* 11 (9): 2477–2501.
- Cloern, J.E., C. Grenz, and L. Videgar-Lucas. 1995. An empirical model of the phytoplankton chlorophyll: Carbon ratio-the conversion factor between productivity and growth rate. *Limnology and Oceanography* 40 (7): 1313–1321.
- Cloern, J.E., K.A. Hieb, T. Jacobson, B. Sansó, E. Di Lorenzo, M.T. Stacey, J.L. Largier, W. Meiring, W.T. Peterson, and T.M. Powell. 2010. Biological communities in San Francisco Bay track large-scale climate forcing over the North Pacific. *Geophysical Research Letters* 37 (21).
- Cloern, J.E., and A.D. Jassby. 2012. Drivers of change in estuarine-coastal ecosystems: discoveries from four decades of study in San Francisco Bay. *Reviews of Geophysics* 50 (4).

- Cloern, J.E., S.M. Safran, L.S. Vaughn, A. Robinson, A.A. Whipple, K.E. Boyer, J.Z. Drexler, R.J. Naiman, J.L. Pinckney, and E.R. Howe. 2021. On the human appropriation of wetland primary production. *Science of the Total Environment* 785: 147097.
- Deines, P. 1980. The isotopic composition of reduced organic carbon. *Limnology and Oceanography* 25: 1499–1502.
- Finlay, J.C., and C. Kendall. 2007. Stable isotope tracing of temporal and spatial variability in organic matter sources to freshwater ecosystems. *Stable Isotopes in Ecology and Environmental Science* 2: 283–333.
- Ganju, N.K., N. Knowles, and D.H. Schoellhamer. 2008. Temporal downscaling of decadal sediment load estimates to a daily interval for use in hindcast simulations. *Journal of Hydrology* 349 (3–4): 512–523.
- Gilbert, G.K. 1917. Hydraulic-mining debris in the Sierra Nevada. US Government Printing Office.
- Greenfield, B.K., G.S. Siemerling, J.C. Andrews, M. Rajan, S.P. Andrews, and D.F. Spencer. 2007. Mechanical shredding of water hyacinth (*Eichhornia crassipes*): Effects on water quality in the Sacramento-San Joaquin River Delta. *California. Estuaries and Coasts* 30 (4): 627–640.
- Harfmann, J., T. Kurobe, B. Bergamaschi, S. Teh, and P. Hernes. 2019. Plant detritus is selectively consumed by estuarine copepods and can augment their survival. *Scientific Reports* 9 (1): 1–9.
- Hernes, P.J., R.Y. Dyda, and B.A. Bergamaschi. 2020. Reassessing particulate organic carbon dynamics in the highly disturbed San Francisco Bay Estuary. *Frontiers in Earth Science* 8: 185.
- Hestir, E.L., D.H. Schoellhamer, J. Greenberg, T. Morgan-King, and S.L. Ustin. 2016. The effect of submerged aquatic vegetation expansion on a declining turbidity trend in the Sacramento-San Joaquin River Delta. *Estuaries and Coasts* 39 (4): 1100–1112.
- Hestir, E.L., D.H. Schoellhamer, T. Morgan-King, and S.L. Ustin. 2013. A step decrease in sediment concentration in a highly modified tidal river delta following the 1983 El Niño floods. *Marine Geology* 345: 304–313.
- Hirsch, R.M. 2014. Large biases in regression-based constituent flux estimates: Causes and diagnostic tools. *JAWRA Journal of the American Water Resources Association* 50 (6): 1401–1424.
- Hirsch, R.M., D.L. Moyer, and S.A. Archfield. 2010. Weighted regressions on time, discharge, and season (WRTDS), with an application to Chesapeake Bay river inputs 1. *JAWRA Journal of the American Water Resources Association* 46 (5): 857–880.
- Hixson, S.M., B. Sharma, M.J. Kainz, A. Wacker, and M.T. Arts. 2015. Production, distribution, and abundance of long-chain omega-3 polyunsaturated fatty acids: A fundamental dichotomy between freshwater and terrestrial ecosystems. *Environmental Reviews* 23 (4): 414–424.
- Hollibaugh, J.T., P.S. Wong, and M.C. Murrell. 2000. Similarity of particle-associated and free-living bacterial communities in northern San Francisco Bay. *California. Aquatic Microbial Ecology* 21 (2): 103–114.
- Jaffe, B., R.E. Smith, and L.Z. Torresan. 1998. Sedimentation and bathymetric change in San Pablo Bay, 1856–1983, Geological Survey.
- Jaffe, B.E., R.E. Smith, and A.C. Foxgrover. 2007. Anthropogenic influence on sedimentation and intertidal mudflat change in San Pablo Bay, California: 1856–1983. *Estuarine, Coastal and Shelf Science* 73 (1–2): 175–187.
- Jassby, A.D., and J.E. Cloern. 2010. wq: Some tools for exploring water quality monitoring data. R package version 0.2–2.
- Kendall, C., and J.J. McDonnell. 2012. *Isotope tracers in catchment hydrology*. Elsevier.
- Kendall, C., S.R. Silva, and V.J. Kelly. 2001. Carbon and nitrogen isotopic compositions of particulate organic matter in four large river systems across the United States. *Hydrological Processes* 15 (7): 1301–1346.
- Krone, R.B. 1979. Sedimentation in the San Francisco bay system. San Francisco Bay: the urbanized estuary, 85–96.
- Livsey, D.N., M.A. Downing-Kunz, D.H. Schoellhamer, and A. Manning. 2021. Suspended-sediment flux in the San Francisco Estuary; Part II: The impact of the 2013–2016 California drought and controls on sediment flux. *Estuaries and Coasts* 44 (4): 972–990.
- McKee, L., M. Lewicki, D.H. Schoellhamer, and N.K. Ganju. 2013. Comparison of sediment supply to San Francisco Bay from watersheds draining the Bay Area and the Central Valley of California. *Marine Geology* 345: 47–62.
- McKee, L.J., N.K. Ganju, and D.H. Schoellhamer. 2006. Estimates of suspended sediment entering San Francisco Bay from the Sacramento and San Joaquin Delta, San Francisco Bay. *California. Journal of Hydrology* 323 (1–4): 335–352.
- Middelburg, J.J., and P.M. Herman. 2007. Organic matter processing in tidal estuaries. *Marine Chemistry* 106 (1–2): 127–147.
- Moyer, D., R.M. Hirsch, and K. Hyer. 2012. Comparison of two regression-based approaches for determining nutrient and sediment fluxes and trends in the Chesapeake Bay watershed. US Geological Survey.
- Müller-Solger, A.B., A.D. Jassby, and D.C. Müller-Navarra. 2002. Nutritional quality of food resources for zooplankton (*Daphnia*) in a tidal freshwater system (Sacramento-San Joaquin River Delta). *Limnology and Oceanography* 47 (5): 1468–1476.
- Murrell, M., J. Hollibaugh, M. Silver, and P. Wong. 1999. Bacterioplankton dynamics in northern San Francisco Bay: Role of particle association and seasonal freshwater flow. *Limnology and Oceanography* 44 (2): 295–308.
- Pondell, C.R., Y. Feng, D.J. Detweiler, and E.A. Canuel. 2020. *Recent changes in organic carbon and food resources in response to environmental change in the Sacramento-San Joaquin Delta*, B052-0010. USA: California.
- Schoellhamer, D., L. McKee, S. Pearce, P. Kauhanen, M. Salomon, S. Dusterhoff, L. Grenier, M. Marineau, and P. Trowbridge. 2018. Sediment supply to San Francisco Bay, Water Years 1995 through 2016: data, trends, and monitoring recommendations to support decisions about water quality, tidal wetlands, and resilience to sea level rise. Published by San Francisco Estuary Institute (SFEI), Richmond, CA. SFEI Contribution (842).
- Schoellhamer, D.H. 2011. Sudden clearing of estuarine waters upon crossing the threshold from transport to supply regulation of sediment transport as an erodible sediment pool is depleted: San Francisco Bay, 1999. *Estuaries and Coasts* 34 (5): 885–899.
- Schoellhamer, D.H., N.K. Ganju, and G.G. Shellenbarger. 2008. Sediment transport in San Pablo Bay. Technical studies for the aquatic transfer facility: Hamilton wetlands restoration project, 36–107.
- Schrage, T.S., and J.E. Cloern. 2017. Water quality measurements in San Francisco Bay by the US Geological Survey, 1969–2015. *Scientific Data* 4 (1): 1–14.
- Sobczak, W.V., J.E. Cloern, A.D. Jassby, B.E. Cole, T.S. Schrage, and A. Arnsberg. 2005. Detritus fuels ecosystem metabolism but not metazoan food webs in San Francisco estuary's freshwater Delta. *Estuaries* 28 (1): 124–137.
- Ta, J., L.W. Anderson, M.A. Christman, S. Khanna, D. Kratville, J.D. Madsen, P.J. Moran, and J.H. Viers. 2017. Invasive aquatic vegetation management in the Sacramento–San Joaquin River Delta: status and recommendations. *San Francisco Estuary and Watershed Science* 15(4).
- Wakeham, S., and E.A. Canuel. 2016. The nature of organic carbon in density-fractionated sediments in the Sacramento-San Joaquin River Delta (California). *Biogeosciences* 13 (2): 567–582.

- Ward, N.D., T.S. Bianchi, P.M. Medeiros, M. Seidel, J.E. Richey, R.G. Keil, and H.O. Sawakuchi. 2017. Where carbon goes when water flows: Carbon cycling across the aquatic continuum. *Frontiers in Marine Science* 4: 7.
- Wright, S.A., and D.H. Schoellhamer. 2004. Trends in the sediment yield of the Sacramento River, California, 1957–2001. *San Francisco Estuary and Watershed Science* 2(2).
- Wright, S.A., and D.H. Schoellhamer. 2005. Estimating sediment budgets at the interface between rivers and estuaries with application to the Sacramento-San Joaquin River Delta. *Water Resources Research* 41(9).